A Study on the Effect of RF Termination Type on Distortion in a Multiband Power Amplifier

Adam Der
Dept. of Electrical, Computer & Energy Engineering
University of Colorado Boulder
Boulder, CO USA
adam.der@colorado.edu

Taylor Barton
Dept. of Electrical, Computer & Energy Engineering
University of Colorado Boulder
Boulder, CO USA
taylor.w.barton@colorado.edu

***Abstract*—This work describes the design and measured comparison of two 28-GHz MMIC power amplifiers (PAs) which are identical except for a difference in how the quarter-wavelength transmission line of the bias tee is terminated. The purpose of the presented study is to compare the effects of this termination on distortion of the PA output signal. In particular, the structure isolates a specific aspect of a dual-band or frequency-reconfigurable PA. Both MMICs are measured in CW and for modulated (2-tone) signals and demonstrate a saturated output power of 30 dBm with >30% measured PAE.**

***Index Terms*—dual-band, GaN, power amplifier**

I. Introduction

Dual-band and multi-band RF front-ends are increasingly needed for carrier-aggregation and multi-use front-end requirements. This requirement has driven the development of dual-band power amplifiers (PAs) that can operate either by reconfiguration or at multiple frequencies simultaneously [1]–[5]. In addition to needing to meet the standard RF performance parameters as for single-band PAs, multi-band solutions may also face additional challenges in linearity [1], [2].

In prior work we have presented a PA design methodology in which the matching network designs at two different operating frequencies are decoupled from each other. In other words, the higher-frequency matching network can be designed first and fully optimized before the lower-frequency matching network is realized. This technique, shown in simplified form in Fig. 1, avoids the back-and-forth design iteration required in many other multi-band techniques. In [4] the architecture is implemented as a frequency-reconfigurable network, in which a transistor switch selects the band. In the concurrent dual-band demonstration in [5], the frequency-dependent short circuit for band selection is instead implemented using a capacitor, which appears as an RF short at the higher operating band and is integrated into the impedance matching network at the lower band.

Selecting a frequency-reconfigurable vs. dual-band design approach depends on various system goals including whether concurrent multi-band operation is required, on the availability of a low-loss RF switch [6], and on the separation in frequency of the two operating bands (for which the fixed capacitor solution has limitations). A further consideration that is the focus of this paper is the topology's effect on distortion. While in principle the location of the switch / capacitor terminating device at the end of a quarter-wavelength transmission line means that it should not have a large effect on linearity, it is well-known that the output capacitance of a transistor is nonlinear [7] and therefore the switch implementation may introduce distortion.

The authors thank WIN Semiconductors for the fabrication of the GaN MMICs described in this work.

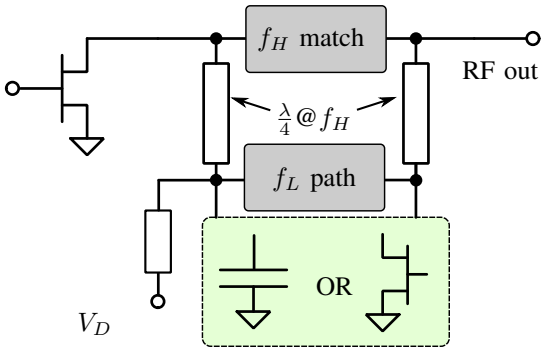

Fig. 1: Simplified schematic of the reconfigurable (switch version) or dual-band (capacitor version) matching network for multi-function PAs studied in this work.

To isolate this specific effect, this work compares two PA MMICs that embody the simplest version of one path of the reconfigurable PA structure of [4], [5]. We present CW and modulated measurements to study the effect of this termination on linearity in a direct, measured comparison.

II. Theory and Design

The technical approach that is the basis for this study is shown in Fig. 1. In this dual-band matching network design technique, transmission lines that are a quarter-wavelength long at the higher band (f_H) are used to isolate the design of the f_H signal path from the lower-frequency (f_L) path. In a switch-based implementation [4], a single transistor switch in parallel with an optional shunt impedance performs frequency reconfiguration: with the switch closed, only the f_H path is available and the high-frequency impedance looking into the transmission lines appears as an open; with the switch open, the entire network provides an impedance match for the

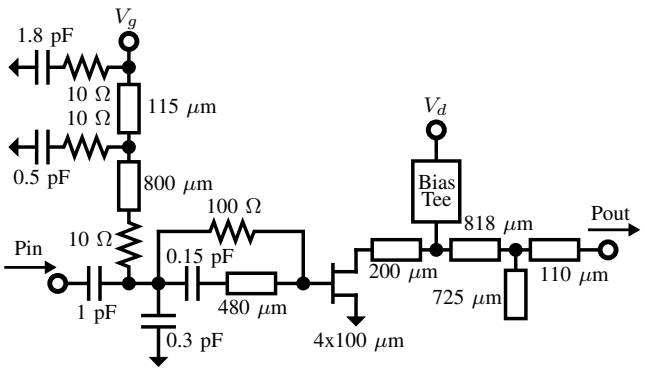

Fig. 2: Simplified schematic of the PAs' excluding the two different bias-tees that can be seen in Fig. 3.

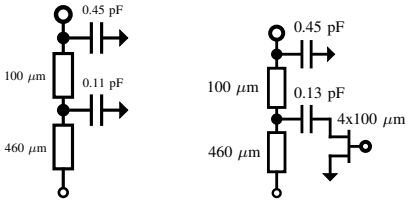

Fig. 3: Schematic of the (a) bias-tee with only passive elements, and (b) bias-tee what uses a device in series to ground the capacitor.

f_L band. In a capacitor-based implementation [5], the switch is replaced with a shunt capacitor on each side of an f_L impedance match, with the capacitors functioning as a shorted impedance at the upper frequency and as part of the impedance match at the lower frequency. In each version, the $\lambda_H/4$ lines furthermore function as a bias structure at the upper band.

To specifically evaluate whether the choice of a capacitor-based or a switch-based termination on the $\lambda_H/4$ transmission line has an effect on linearity, in this work we have designed two MMIC PAs with nearly identical structures as shown schematically in Fig. 2. In order to isolate performance differences to the $\lambda_H/4$ transmission line only, the designs represent only the f_H path of the generalized diagram in Fig. 1, i.e. they are single-frequency designs. In case 1, the line is terminated by a 0.11 pF fixed capacitor, and in case 2 it is terminated by a 0.13 pF capacitor in series with a 4x100 μm transistor switch. The two different bias structures are shown in detail in Fig. 3.

The circuits are fabricated using the WIN Semiconductors NP12-01 GaN-on-SiC technology targeting mm-wave power applications through 50GHz. This 0.12 μm gate process is manufactured on 100mm SiC substrates and uses a source-coupled field plate design to provide high breakdown voltage required for reliable operation at $V_{ds} = 28$ V. 4x50 μm transistors exhibit typical Psat of 4W/mm, 13.5 dB linear gain and drain efficiency over 50% at 29 GHz. The NP12-01 platform supports multiple MMIC functions with PA/LNA/SW optimized transistor layouts, two interconnect metal layers,

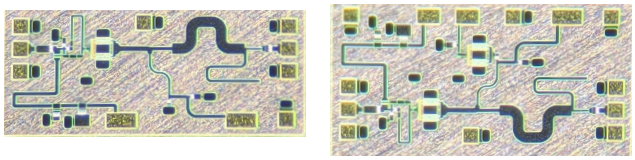

(a) (b)

Fig. 4: Photographs of the fabricated MMICs: (a) passive match (1.9 x 0.8 mm^2) and (b) match with transistor in OMN (1.9 x 0.9 mm^2).

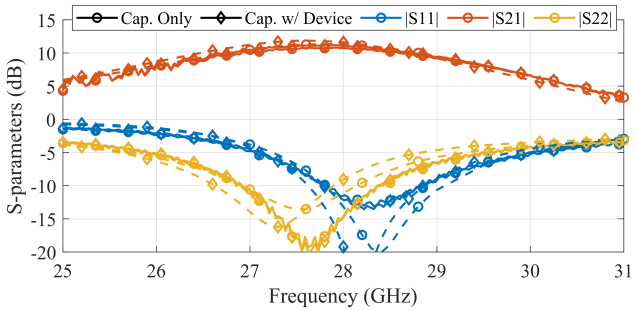

Fig. 5: S-parameter measurement and simulation comparison for the two designs.

high reliability MIM capacitors, precision TaN resistors and through wafer vias for low-inductance grounding. Photographs of the fabricated MMICs are shown in Fig. 4.

III. MMIC Measurements

The MMIC PAs were mounted on CuMo carriers with 100 pF and 10 μF off-chip capacitance on the gate and drain. For the measurements presented in this work the RF input and outputs are probed. S-parameter measurements are made using a Rohde & Schwarz ZNA67 and CW and modulated measurements are performed using a testbench based on a Rohde & Schwarz SMW200A RF signal generator, FSW43 signal analyzer, and power meters.

In Fig. 5, the measured and simulated S-parameters are compared for the two PA designs. Although agreement is overall very close, the measured 10.5 dB small-signal gain of both PAs is slightly lower than the expected 11 dB. Return loss remains below -12 dB in measurement. Large-signal CW measurements are shown in Fig. 6. A table comparing these results to state-of-the-art GaN MMIC PAs is included in Table I.

Finally, to evaluate the nonlinearity of the two designs the MMICs are characterized under a two-tone input signal over tone spacing at a fixed input power of 14 dBm [Fig. 7], over power at a fixed 100 MHz tone spacing at 28 GHz [Fig. 8]. The nonlinearities were also compared using a 100 MHz LTE-like signal and adjusting the gate bias voltage of the switch transistor [Fig. 9]. Both the two-tone signals with tone spacings up to 100 MHz and LTE-like signals show better linearity for the passive termination case. At a 200 MHz

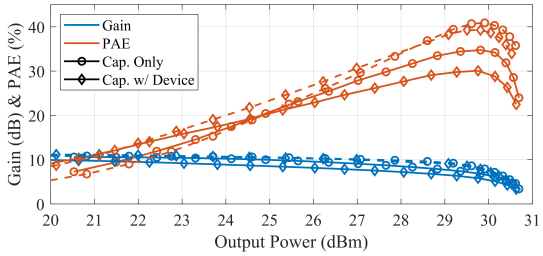

Fig. 6: Simulated and measured large-signal CW performance.

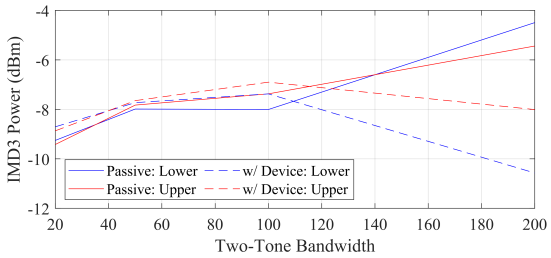

Fig. 7: Measured 2-tone comparison over frequency spacing.

tone spacing, this pattern diverges and the passive-terminated MMIC has a better IMD3.

IV. Conclusion

This work explores the effect of a switch-based termination as used in frequency-reconfigurable PA design on distortion. While there are many factors that may lead to the selection of a fixed dual-band or frequency-reconfigurable PA architecture, one that has not previously been studied in depth is distortion when only one band is in use. The MMIC topologies compared in this work have been designed to isolate this specific effect, while also demonstrating comparable performance to the state of the art. Based on a two-tone characterization of the two MMICs, we find that the passive termination has performance benefits for modulated signals with lower bandwidth while the larger effective capacitance of the active device termination improves its linearity for wider bandwidths, even despite the fact that the capacitance itself has a greater inherent nonlinearity.

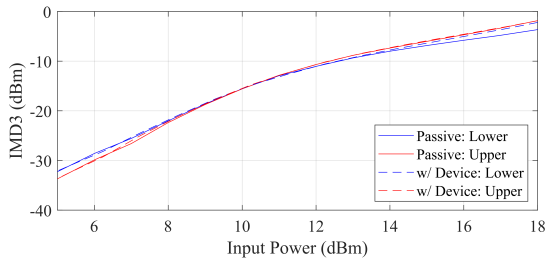

Fig. 8: Measured 2-tone comparison over power at a fixed 100 MHz tone spacing at 28 GHz center frequency.

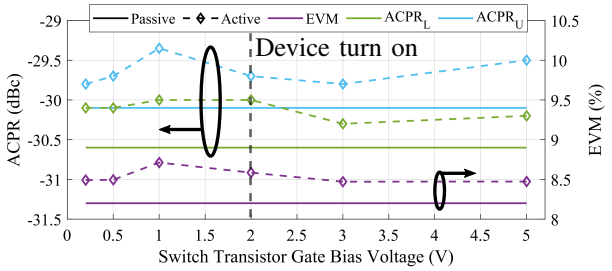

Fig. 9: Measured 100 MHz LTE-like signal with a PAPR of 10 dB and input power held at 14.2 dBm. Comparison between the two PAs while adjusting the gate bias point of the switch.

TABLE I: Comparison to state-of-the-art MMIC PAs.

Ref	Freq (GHz)	Pout (dBm)	Gain (dB)	PAE (%)	Size (mm2)
[4]	2.6-7.3 /17.4-23	20.1/ 20.7	7.3/ 4.5	29.5/ 27.2	1.4 x 2.4
[5]	4.3-6.3/ 26.1-31	31-32.5/ 30-31	12.5-14.5/ 13.4-13.7	22-23/ 22-24.3	2.7 x 3
[8]	25-29/ 25-29	10.5/ 20	13-18/ 10-12	28-32/ 25-30	13.8/ 23.8
[9]	26.5-31	41.9	18-22	16.1- 20.3	4.5x 6.4
[10]	29.5	34	28	34	11.7
This work	28	30.7	6-7	35 / 30	1.9 x 0.8/ 1.9 x 0.9

References

[1] M. Taguchi, Y. Komatsuzaki, K. Nakatani, and S. Shinjo, "An arbitrary order IMD suppression method for dual-input power amplifiers by controlling the phase differences of dual-band signals," in *Asia-Pacific Microwave Conference (APMC)*, 2023, pp. 19–21.

[2] W. Sear, N. Biesterfeld, S. Bayaskar, and T. Barton, "An inter-stage filter network for distortion reduction in concurrent dual-band power amplifier operation," in *Asia-Pacific Microwave Conference (APMC)*, 2022, pp. 503–505.

[3] J.-X. Chou and Y.-S. Lin, "Novel concurrent dual-band power amplifier design using a bridged-T coil-based impedance matching network," in *Asia-Pacific Microwave Conference (APMC)*, 2023, pp. 515–517.

[4] A. Der *et al.*, "A S-C- / K-band reconfigurable GaAs MMIC power amplifier for 5G applications," in *IEEE MTT-S International Microwave Symposium*, 2021, pp. 873–876.

[5] A. T. Der and T. W. Barton, "C/Ka concurrent dual-band GaN MMIC based on shorted quarter-wavelength line topology," *IEEE Journal of Microwaves*, pp. 1–9, 2024.

[6] A. Der, W. Sear, and T. Barton, "Effect of switch figure of merit on frequency-reconfigurable power amplifier performance," in *European Microwave Conference (EuMC)*, 2022, pp. 954–957.

[7] Z. A. Mokhti *et al.*, "The nonlinear drain–source capacitance effect on continuous-mode class-B/J power amplifiers," *IEEE Transactions on Microwave Theory and Techniques*, vol. 67, no. 7, pp. 2741–2747, 2019.

[8] K. Nakatani, Y. Yamaguchi, M. Hangai, and S. Shinjo, "A ka-band cw 15.5w 15.6

[9] S. Samis *et al.*, "Broadband high-efficiency power amplifiers in 150 nm algan/gan technology at ka-band," in *2020 IEEE Asia-Pacific Microwave Conference (APMC)*, 2020, pp. 260–262.

[10] C. F. Campbell, Y. Liu, M.-Y. Kao, and S. Nayak, "High efficiency ka-band gallium nitride power amplifier mmics," in *2013 IEEE International Conference on Microwaves, Communications, Antennas and Electronic Systems (COMCAS 2013)*, 2013, pp. 1–5.